The Journal of Neuroscience, July 1, 1999, *19*(13):5195–5204

A Zinc-Dependent Cl^- Current in Neuronal Somata

Toshihide Tabata and Andrew T. Ishida

Section of Neurobiology, Physiology, and Behavior, University of California, Davis, California 95616-8519

Extracellular Zn^{2+} modulates current passage through voltage- and neurotransmitter-gated ion channels, at concentrations less than, or near, those produced by release at certain synapses. Electrophysiological effects of cytoplasmic Zn^{2+} are less well understood, and effects have been observed at concentrations that are orders of magnitude greater than those found in resting and stimulated neurons. To examine whether and how neurons are affected by lower levels of cytoplasmic Zn^{2+}, we tested the effect of Zn^{2+}-selective chelators, Zn^{2+}-preferring ionophores, and exogenous Zn^{2+} on neuronal somata during whole-cell patch-clamp recordings. We report here that cytoplasmic zinc facilitates the downward regulation of a background Cl^- conductance by an endogenous protein kinase C (PKC) in fish retinal ganglion cell somata and that this regulation is maintained if nanomolar levels of free Zn^{2+} are available. This regulation has not been described previously in any tissue, as other Cl^- currents have been described as reduced by PKC alone, reduced by Zn^{2+} alone, or reduced by both independently. Moreover, control of cation currents by a zinc-dependent PKC has not been reported previously. The regulation we have observed thus provides the first electrophysiological measurements consistent with biochemical measurements of zinc-dependent PKC activity in other systems. These results suggest that contributions of background Cl^- conductances to electrical properties of neurons are susceptible to modulation.

Key words: background chloride conductance; resting potential; outward rectification; PKC; Zn^{2+}; divalent cation

Calcium, magnesium, and zinc are found in both bound and ionized forms in neuronal and muscle cytoplasm. Of these, the concentration and physiological effects of unbound intracellular calcium (Ca^{2+}) have been studied most extensively. Fluorescent indicators and patch-clamp methods have shown substantial agreement between the endogenous free Ca^{2+} levels measured during certain electrophysiological responses and buffered levels of exogenous Ca^{2+} that can elicit those events (e.g., Johnson and Byerly, 1993; Roberts, 1993; Burgoyne and Morgan, 1995; Etter et al., 1996). Recent measurements suggest a similar correlation for Mg^{2+}, in that free intracellular Mg^{2+} concentrations range from 0.6 to 5 mM (Brocard et al., 1993) and thus span the range of Mg^{2+} levels that gate or regulate ion channels (e.g., Matsuda et al., 1987; Stelzer et al., 1988; Johnson and Ascher, 1990; O'Rourke et al., 1992). By comparison, electrophysiological effects of cytoplasmic Zn^{2+} have been reported rarely, and these effects have been obtained with Zn^{2+} concentrations that are several orders of magnitude greater than the picomolar-to-micromolar levels found in recent histochemical studies (Begenisich and Lynch, 1974; Woll et al., 1987; Frederickson, 1989; Kokubun et al., 1991; Groschner and Kukovetz, 1992; Staley, 1994; Lascola et al., 1998; Sensi et al., 1997). We therefore tested whether and how neurons are affected electrophysiologically by lower concentrations of cytoplasmic Zn^{2+} and by changes in these levels. For this purpose, we applied various combinations of Zn^{2+}, Zn^{2+}-selective chelators, and Zn^{2+}-preferring ionophores to isolated neuronal somata during perforated- and ruptured-patch whole-cell patch-clamp recordings. We specifically tested for these effects in neurons that contain protein kinase C (PKC) (cf. Cuenca et al., 1990; Osborne et al., 1992), because biochemical studies have shown that Zn^{2+} binds PKC and facilitates its activity at submicromolar concentrations (Murakami et al., 1987; Csermely et al., 1988; Sekiguchi et al., 1988; Forbes et al., 1991; Hubbard et al., 1991). We present evidence here that intracellular zinc facilitates the reduction of a "background" Cl^- conductance (Franciolini and Petris, 1990) by an endogenous PKC in retinal ganglion cells.

The results below are presented in two parts. The first identifies an outwardly rectifying Cl^- current that constitutes a background Cl^- conductance in retinal ganglion cells. The second part provides evidence that regulation of this current by endogenous PKC is zinc dependent.

Portions of these data have appeared in a meeting abstract (Tabata and Ishida, 1997).

MATERIALS AND METHODS

Whole-cell recordings. The voltage-clamp currents described here were measured in single, neurite-free retinal ganglion cell somata isolated from adult common goldfish (*Carassius auratus*). Cells were isolated and identified as described elsewhere (see Bindokas et al., 1994; Tabata and Ishida, 1996; Hidaka and Ishida, 1998). Currents were measured in tight-seal whole-cell configurations, in either ruptured- or perforated-patch mode (Hamill et al., 1981; Horn and Marty, 1988). Experiments were performed at ~23°C within 20 hr of cell isolation, using borosilicate glass pipettes with tip resistances of 2–3 MΩ and an Axopatch-1D amplifier (Axon Instruments, Foster City, CA).

During recording, cells were continuously superfused with a control bath solution (see below) at a rate of 1.2 ml/min. To reduce the time required to change extracellular solution composition and to ensure that current changes were not attributable to mechanical artifacts, we applied control and test solutions sequentially to cells, either by switching be-

Received Feb. 24, 1999; revised April 8, 1999; accepted April 12, 1999.

This work was supported by National Institutes of Health Grant EY 08120 from the National Eye Institute (Bethesda, MD) to A.T.I. We thank Professor Philippe Ascher for helpful criticism of this manuscript, Professors Yutaka Fukuda and Masanobu Kano for the opportunity to pursue this study, and Ms. Gloria Partida for preparing the primary cell cultures used in these experiments.

Correspondence should be addressed to Dr. Andrew T. Ishida, Section of Neurobiology, Physiology, and Behavior, University of California, One Shields Avenue, Davis, CA 95616-8519.

Dr. Tabata's present address: Department of Physiology, Kanazawa University School of Medicine, Kanazawa, Ishikawa 920–8640, Japan.

tween fluid reservoirs fed into a microperfusion U-tube or by shifting the position of a parallel array of glass tubes that each superfused a different solution over the cells being recorded. As described elsewhere (Tabata and Ishida, 1996), command potential generation, data storage, and off-line analysis were performed with pCLAMP software (version 6.0.3; Axon Instruments); capacitive currents were reduced as much as possible by use of the cancellation circuitry of the amplifier; current signals were analog-filtered at 1 kHz and digitally sampled at 2 kHz; and liquid junction potentials between pipette and bath solutions were measured and corrected for before data collection. Membrane potentials are reported without compensation for series resistance (mean ± SEM; 18 ± 1 MΩ in ruptured-patch mode; $n = 65$; 32 ± 4 MΩ in perforated-patch mode; $n = 46$) because the total membrane current rarely exceeded 200 pA. Unless otherwise indicated, data are reported here as mean values ± 1 SEM from the indicated number (n) of cells. The current amplitudes reported are the mean values recorded during the final 20 msec of 100 msec steps to each test potential. Changes in current amplitudes measured under various conditions were compared by Wilcoxon rank-sum tests because these values did not distribute normally. Variances of data measured with different pipette solutions (e.g., see Fig. 3*C*) were compared by F tests (by comparing the ratio of the variances).

Solutions. The compositions of the routinely used pipette and bath solutions are as follows (exceptions are noted in the figure legends). In ruptured-patch mode, the 30 nM Zn^{2+}-containing pipette solution consisted of (in mM): 150 *N*-methyl-D-glucamine (NMDG), 0.226 $CaCl_2$, 1.7 $MgCl_2$, 3.6 $ZnCl_2$, 2 ATP-Mg, 4 EGTA, and 5 HEPES. The Cl^- concentration in this solution (11 mM) was used for the comparison of equilibrium and reversal potentials (see Fig. 2). The Zn^{2+}-free pipette solution contained (in mM): 150 NMDG, 2.48 $CaCl_2$, 1.73 $MgCl_2$, 2 ATP-Mg, 4 EGTA, and 5 HEPES. The Zn^{2+}-free and Zn^{2+}-containing pipette solutions contained different amounts of total Ca^{2+} but identical amounts of calculated free Ca^{2+} (see below). The pH of both of these solutions was adjusted to 7.5 with D-gluconic acid (DGA). In some experiments, the PKC catalytic subunit (#539513; Calbiochem, La Jolla, CA), and PKC[19–31] (#1443 976; Boehringer Mannheim, Indianapolis, IN) were first dissolved into water to a concentration 1000 times higher than the final one and then diluted into the Zn^{2+}-free pipette solution to the final concentration immediately before experiments. In perforated-patch mode, the pipette tip was filled with a solution containing (in mM): 150 CsOH, 3.5 $CaCl_2$, 4 $MgCl_2$, 10 BAPTA, and 5 HEPES; pH was adjusted to 7.5 with DGA. The pipette shank was filled with the above solution mixed at 500:1 with a solution of 3.3% (w/v) amphotericine B (Sigma, St. Louis, MO) and 10% (w/v) pluronic (P-1572; Molecular Probes, Eugene, OR) in DMSO.

The concentrations of free divalent cations in each pipette solution (reported in the text and each figure legend) were calculated using the equations in Chang et al. (1988) and the stability constants in Smith and Martell (1975) corrected for ionic equivalent, pH, and temperature according to the method of Marks and Maxfield (1991). EGTA was used instead of BAPTA in these experiments, because dissociation constants for the binding of Zn^{2+} by BAPTA are not available. In the cases of Zn^{2+}-free solutions, the free Ca^{2+} and Mg^{2+} values calculated as described above did not differ by >20% from those calculated using the Bound and Determined software (Brooks and Storey, 1992) implementing the method of Marks and Maxfield (1991). Unless stated otherwise, the free Ca^{2+} concentration in all pipette solutions was set to levels detected in resting retinal ganglion cells by fura-2 fluorescence intensity [100 nM (Bindokas et al., 1994)]. The free Zn^{2+} concentration in the pipette solution routinely used for ruptured-patch recordings (30 nM) was selected because it falls within the range of concentrations measured in a variety of intact cells (cf. Sensi et al., 1997) and because micromolar Zn^{2+} has consistently been found to inhibit PKC activity in biochemical studies (Murakami et al., 1987; Csermely et al., 1988; Sekiguchi et al., 1988). We know of no method that could have been used during the ruptured-patch recordings reported here to demonstrate the precise distribution and concentration of Zn^{2+} established in the cell cytoplasm by exchange with the pipette solution.

The standard bath solution contained (in mM): 105 Na-DGA, 18 NaCl, 0.001 tetrodotoxin (TTX), 0.1 $CaCl_2$, 2.4 $CoCl_2$, 30 tetraethylammonium (TEA)-Cl, 3 4-aminopyridine (4-AP), 10 D-glucose, and 5 HEPES; pH was adjusted to 7.5 with NaOH and/or HCl. To prepare a test bath solution, we first dissolved a test agent into an appropriate vehicle solvent to a concentration 1000 times higher than the concentration to be applied. This stock solution was kept at −30°C for up to 1 week and diluted into the bath solution to the final concentration immediately before experiments. The following solvents were used: water for Rp-cAMP (Calbiochem) and pyrithione-Na (Aldrich, Milwaukee, WI); ethanol for *N,N,N′,N′*-tetrakis-(2-pyridylmethyl)-ethylenediamine (TPEN; Calbiochem); methanol for 4,4′-di-isothiocyanostilbene-2,2′-disulfonic acid (DIDS; Aldrich) and 4-acetamido-4′-isothiocyanostilbene-2–2′-disulfonic acid (SITS; Aldrich); and DMSO for bisindolylmaleimide I (Calbiochem), calphostin C (Calbiochem), and 4-bromo-A23187 (4-BrA23187; Calbiochem). The control bath solution contained the same vehicle solvent as the corresponding test bath solution.

Three precautions were exercised routinely during this study. First, the ruptured-patch pipette solution, the perforated-patch pipette solution, and bath solutions were adjusted with sucrose to 320 ± 5, 330 ± 5, and 330 ± 5 mOsm/kg, respectively. With these osmolalities, neither swelling nor shrinkage of cells occurred after giga-seal formation. Second, DIDS-sensitive current was measured in individual cells by digital subtraction of currents recorded before and during a single application of DIDS, because multiple applications irreversibly altered the kinetics and degree of I_{Cl} deactivation in many cells and because retinal ganglion cells possess a K^+ current (I_B) that resists block by TEA, 4-AP, and Cs^+ (Lukasiewicz and Werblin, 1988; Sucher and Lipton, 1992). Changes of I_{Cl} amplitude produced by pharmacological treatments that augment or block PKC activity were gauged either with a single DIDS application at the end of an experiment or by comparison of the reversal potential and kinetics of the difference between currents recorded before and during the pharmacological treatments. Third, voltage-gated cation currents were suppressed as follows: Na^+ current was blocked by inclusion of 1 μM TTX, Ca^{2+} currents were blocked by 2.4 mM Co^{2+} and reduced Ca^{2+} (0.1 mM), K^+ currents (except I_B) were blocked by 30 mM TEA and 3 mM 4-AP, and hyperpolarization-activated cation current (I_h) was suppressed by excluding K^+ from the bath solution (see Bindokas et al., 1994; Tabata and Ishida, 1996; Hidaka and Ishida, 1998).

RESULTS

In the presence of pharmacological blockers of voltage-gated Na^+, K^+, and Ca^{2+} currents (TTX, TEA^+, 4-AP, and Co^{2+}), depolarization of retinal ganglion cell somata activated an outwardly rectifying current whose amplitude was reduced by agents that block voltage-gated Cl^- current in other tissues. This current appeared to be carried by Cl^- ions—and will be referred to hereafter as I_{Cl}—because its reversal potential shifted with the chloride equilibrium potential (E_{Cl}) calculated from the Cl^- ion concentrations in the bath and pipette solutions used. A current with similar voltage sensitivity and pharmacological properties was also recorded when Na^+ and K^+ in the bath and recording pipette solutions were replaced by NMDG and TEA^+. I_{Cl} activated in every cell from which we recorded, in ruptured- as well as perforated-patch recording modes ($n = 65$ and 51, respectively). When activated by 100 msec depolarizations from holding potentials between −90 and −70 mV, to test potentials between −80 and +40 mV, I_{Cl} displayed the following pharmacological properties and voltage sensitivity.

Pharmacology

Several Cl^- channel blockers were tested, and total whole-cell current (between −80 and +40 mV) was reduced in amplitude by extracellular application of DIDS ($n = 61$; e.g., Fig. 1*A*) and furosemide (data not shown). This reduction by DIDS and the outward rectification recorded under control conditions (Fig. 1*B*) were not observed if SITS was included in the pipette solution in ruptured-patch mode (consistent with block of the DIDS-sensitive current by intracellular SITS; $n = 6$; Fig. 1*C*,*D*). By contrast, whole-cell current was unaffected by extracellular applications of 100 μM picrotoxinin or 500 nM chlorotoxin ($n = 3$ and 6, respectively; data not shown).

Nearly maximal reduction of the control current amplitude was produced by 1 mM DIDS. The current that resisted block by 1 mM DIDS constituted approximately one-third of the total outward current recorded at a test potential of +40 mV. When normalized

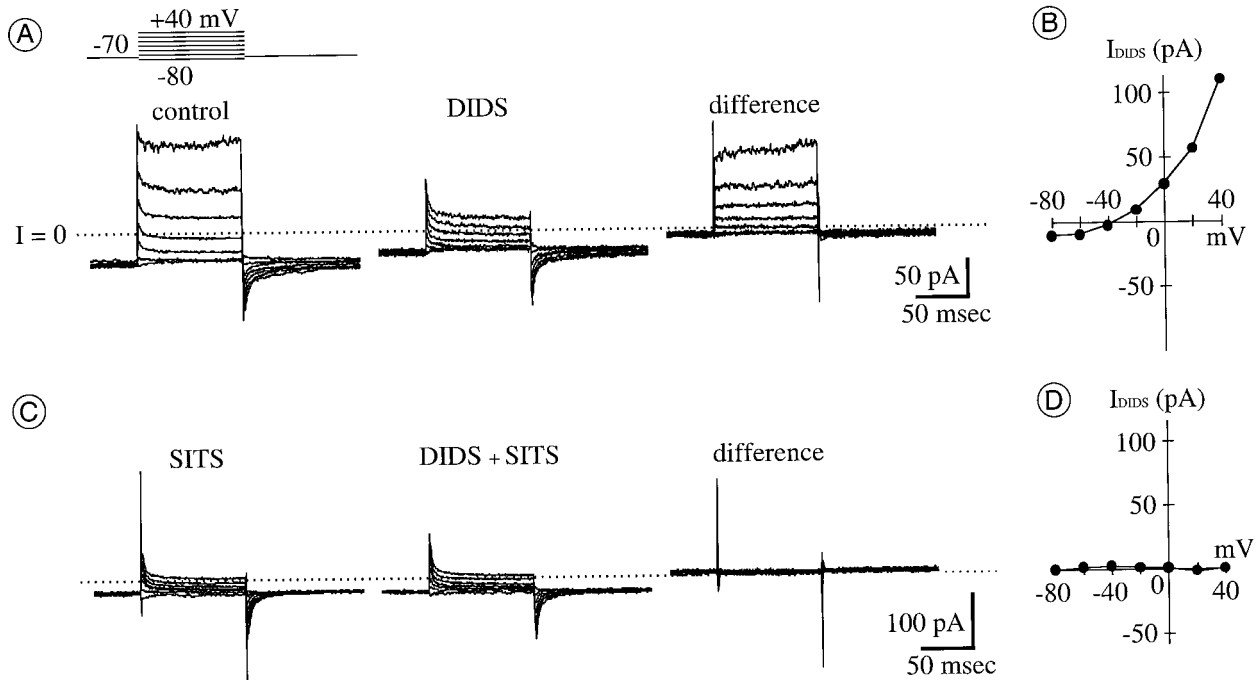

Figure 1. DIDS and SITS reduce an outwardly rectifying current in the presence of Na^+, Ca^{2+}, and K^+ current blockers. *A*, Whole-cell current activated in ruptured-patch mode by the voltage protocol schematically shown *above* current *traces* at *left*. The holding potential (E_{hold}) was −70 mV; test potentials (E_{test}) were from −80 to +40 mV, in 20 mV increments. Currents were recorded before (*left*) and during (*middle*) application of 1 mM DIDS. Subtraction of these currents yields DIDS-sensitive current (*right*). The difference current appears to activate rapidly, not inactivate, and then deactivate rapidly (at onset, plateau, and offset, respectively, of each test depolarization). In this and all other current *traces*, the zero current level is shown by a *dotted line*. *B*, Current–voltage (*I–V*) curve of the DIDS-sensitive current in *A*. In this and all other *I–V* curves, current amplitude is averaged over the final 20 msec of 100 msec steps to each test potential and then plotted against test potential. Current reverses direction near E_{Cl} (−40 mV). *C*, Whole-cell current recorded from a cell different from that in *A* before (*left*) and during (*middle*) application of 1 mM DIDS. Current was activated and recorded as described in *A*, except that 100 μM SITS was included in the recording pipette solution. Ionic current recorded under this condition is unaffected by 1 mM DIDS; the difference between currents before and during DIDS (*right*) is due to slight capacitive current changes only. *D*, *I–V* curve measured from the difference of currents in *C*. The calculated free concentration of Zn^{2+} in the pipette solution ($[Zn^{2+}]_{pip}$) was 30 nM.

to cell capacitance (C_m), the amounts of current that resisted block by DIDS resembled the total whole-cell current recorded (at +40 mV) with pipette solutions that contained 300 μM SITS (0.4 ± 0.4 pA/pF; $n = 6$; see Fig. 1*C*). These DIDS- and SITS-resistant currents were not examined in detail. However, after repolarization to the holding potential, the amplitude of the "tail" of these currents was K^+-sensitive ($n = 31$; data not shown). We presume that this current is analogous to the TEA- and 4-AP–resistant cation current termed I_B in retinal ganglion cells of other species (Lukasiewicz and Werblin, 1988; Sucher and Lipton, 1992) and that it is carried by other cations (primarily Na^+ in ruptured-patch mode and Cs^+ in perforated-patch mode) under our recording conditions, as in other neurons (Zhu and Ikeda, 1993; Callahan and Korn, 1994). This observation indicates that, at the concentrations used, DIDS did not abolish voltage-sensitive currents nonselectively in the cells from which we recorded.

Charge carrier and Ca^{2+} insensitivity

Two results indicated that 1 mM DIDS reduced the amplitude of a Cl^- current in retinal ganglion cells under the recording conditions used here. First, as mentioned above, this current reversed in direction at a membrane potential that shifted with extracellular Cl^- concentration (Fig. 2). When the external Cl^- concentration was changed from 53 to 11 mM (by isosmotic replacement with D-gluconic acid, with the internal Cl^- concentration fixed at 11 mM), the reversal potential of the DIDS-sensitive current shifted from −36 ± 2 mV ($n = 9$) to −3 ± 3 mV ($n = 4$). These results suggest that this current is carried at least primarily by Cl^- ions, as characteristically found in background Cl^- currents of various cells (Franciolini and Petris, 1990). (From the bath and pipette solution compositions, the equilibrium potentials for Na^+ and Ca^{2+} ions are estimated to have been extremely positive values and to have remained constant while the Cl^- reversal potential changed during these measurements.) Second, the reversal potential of the DIDS-sensitive current was unaffected by a 59 mV shift in the H^+ equilibrium potential (produced by 0.5 pH unit increases and decreases in extracellular pH; $n = 6$; Fig. 2). Our records thus showed no detectable amounts of the DIDS-sensitive proton current described in human macrophages (Holevinsky et al., 1994).

Two results indicated that the DIDS-sensitive current was not gated by intracellular Ca^{2+}. First, no increases in current amplitude were detected when cells were exposed to a divalent cation ionophore (4-BrA23187) in the presence of 0.1 mM Ca^{2+} ($n = 5$; see Fig. 5 and its description below). Second, the DIDS-sensitive current density (current amplitude normalized to cell membrane capacitance) did not significantly differ when measured in ruptured-patch mode with pipette solutions containing calculated free Ca^{2+} levels of 10, 30, and 300 nM ($n = 4$, 5, and 3, respectively; data not shown). Although the density of I_{Cl} was indistinguishable when these different pipette solutions were used, the total depolarization-activated outward current density more than doubled at +40 mV (the test potential used routinely to characterize I_{Cl}) when these solutions contained K^+ rather than

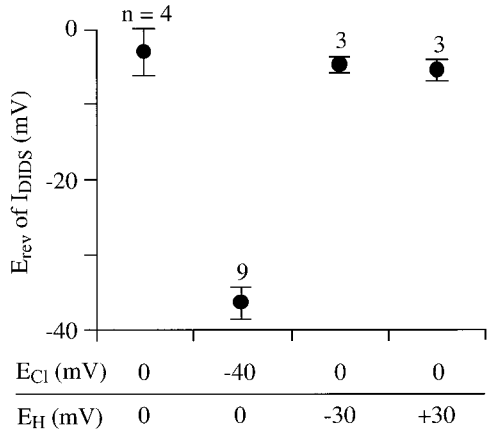

Figure 2. Cl^-, not H^+, carries DIDS-sensitive current. Interpolated values of reversal potential (E_{rev}) of DIDS-sensitive current (measured as described in Fig. 1*B*) listed next to Cl^- and H^+ equilibrium potential values (E_{Cl} and E_H, respectively) set by bath and pipette solution compositions. Ruptured-patch recording mode was used. The control bath solution contained 53 mM Cl^-, the bath Cl^- was reduced to 11 mM by isosmotic replacement with DGA. The pipette solution contained 11 mM Cl^- and 30 nM free Zn^{2+} (see Materials and Methods for other constituents). *Filled circles* and error bars plot the mean ± 1 SEM of E_{rev} measured from the indicated number of cells. E_{rev} of DIDS-sensitive current shifts with E_{Cl} but not with E_H.

NMDG as the major monovalent cation and when the calculated free Ca^{2+} level was increased from 10 to 300 nM. These results are consistent with the presence of a Ca^{2+}-activated K^+ conductance in goldfish retinal ganglion cells, not unlike that suggested by measurements in salamander, turtle, rat, and cat retinal ganglion cells (see Ishida, 1995). By contrast, the activation of the I_{Cl} we report here apparently does not require increases in cytoplasmic Ca^{2+} and thus differs from the Ca^{2+}-activated Cl^- current of rod and cone photoreceptors, retinal bipolar cells, and other central neurons (Bader et al., 1982; Maricq and Korenbrot, 1988; Okada et al., 1995).

On the basis of the above results and to obviate the need for leak-current subtraction, we measured I_{Cl} in the remainder of this study by the difference between whole-cell current recorded before and during application of 1 mM DIDS. The amplitude, reversal potential, and kinetics of I_{Cl} were measured from these "difference currents." In some cases, we also inferred that I_{Cl} was susceptible to regulation by pharmacological agents that affect protein kinase activities, if the difference currents recorded before and during application of these agents resembled the DIDS difference currents.

Gating in ruptured- and perforated-patch modes

The activation range of I_{Cl} included membrane potentials that were more negative and more positive than the E_{Cl} routinely used in our experiments (−40 or −32 mV); I_{Cl} was inward at test potentials more negative than E_{Cl}, and it was outward at more positive test potentials (see Figs. 1*B*, 7*H*). The chord conductance measured from outward currents exceeded that measured from inward currents when the bath and pipette solutions contained equal Cl^- concentrations and when the standard bath and pipette solutions were used (bath, 53 mM Cl^-; pipette, 11 mM Cl^-). When the bath and pipette solutions both contained 11 mM Cl^-, for example, the outward I_{Cl} at +40 mV was 2.9 ± 0.3 (n = 4) times larger in amplitude than the inward I_{Cl} measured at −40 mV.

Over the range of test potentials we routinely used (i.e., between −80 and +40 mV), I_{Cl} did not exhibit markedly time-dependent gating kinetics. First, its rise time was both rapid and not obviously voltage dependent; the rising edge of currents measured after depolarizations to test potentials between −40 and +40 mV could all be fitted by single-exponential time constants of 3–5 msec. Second, I_{Cl} was not detectably inactivated by depolarization because it did not decline in amplitude during sustained depolarizations (Fig. 1) and because the currents activated by depolarizations from −90 to +20 mV were identical in amplitude to those activated by depolarizations from −30 to +20 mV (n = 5; data not shown). Third, tail currents were immeasurably small, and thus I_{Cl} displayed no time-dependent deactivation (Fig. 1).

It was possible to activate I_{Cl} of stable amplitude repeatedly in perforated-patch mode but not in ruptured-patch mode with the standard pipette solution. This was gauged, as explained above, in two steps. The total whole-cell current was measured during the last 20 msec of 100 msec depolarizations, repeated once per 60 sec, from a holding potential of −70 mV to a test potential of +40 mV; 1 mM DIDS was then applied to determine the fraction of the total current that was comprised by I_{Cl}. During ruptured-patch recordings, the amplitude of the total test current increased continuously and by as much as 10-fold or more during the course of 30 min (Fig. 3*A*). We infer that this increase in total whole-cell current is attributable primarily, if not entirely, to increases in I_{Cl} because 1 mM DIDS blocked approximately all of the total current that (by the end of each recording) exceeded the levels recorded at the beginning of each recording (Fig. 3*A*; the possibility that higher concentrations of DIDS might produce larger reductions in the whole-cell current was not tested). During these long-term recordings, the slowly rising current recorded during the first few milliseconds of each test depolarization and the total whole-cell current tail recorded after repolarization to the holding potential did not markedly change in amplitude. These current components therefore vanished upon subtraction of the current traces recorded in the presence and absence of DIDS (Fig. 1), leaving traces that show no time-dependent activation or deactivation (of I_{Cl}). The steady growth of I_{Cl} illustrated by Figure 3*A* was never seen in perforated-patch mode. Instead, the amplitude of the total current decreased within the first 5–10 min of giga-seal formation and was stable thereafter for at least 30 min (Fig. 3*B*). The initial decline in current amplitude presumably reflects the slow replacement of intracellular K^+ by Cs^+ in the pipette solution.

It was technically infeasible to quantify the rate at which I_{Cl} increased over time in ruptured-patch mode by alternating applications of control and DIDS-containing bath solution, because applications of DIDS produced changes in the deactivation kinetics of the total current. Nevertheless, the above results imply that at least some of the current measured during 100 msec test depolarizations may be regulated via an intracellular molecule or mechanism that was lost or compromised by exposure to the ruptured-patch pipette solution. These results also indicate that the slowly rising and tail current components can both be activated repeatedly, without substantial change, in ruptured- as well as perforated-patch recordings.

Regulation of I_{Cl} by a zinc-dependent mechanism

We tested the possibility that the increase in amplitude of I_{Cl} during recordings in ruptured-patch mode resulted from chelation of cytoplasmic Zn^{2+} by EGTA in the pipette solution rather than from chelation of Ca^{2+}. We tested this possibility because

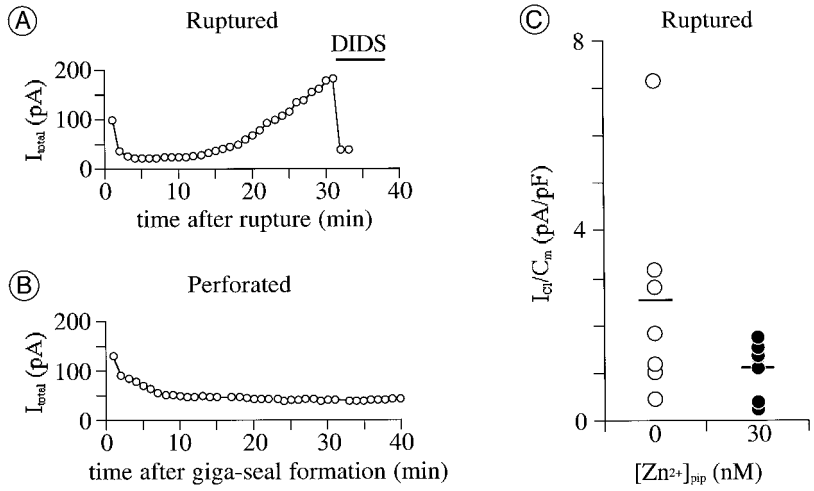

Figure 3. Exogenously supplemented intracellular Zn^{2+} impedes augmentation of I_{Cl} by intracellular perfusion. *A*, *B*, Amplitude of total current at E_{test} of +40 mV plotted against recording time. Recordings in *A* and *B* were in ruptured- and perforated-patch mode, respectively. Pipette solutions in both recordings contained no added zinc ($[Zn^{2+}]_{pip} = 0$); 1 mM DIDS was microperfused onto the cell during the time indicated by the *horizontal bar* in *A*. C_m, 10 pF in *A* and 28 pF in *B*. *C*, I_{Cl} activated by depolarization to +40 mV after 12–15 min of intracellular perfusion with Zn^{2+}-free versus Zn^{2+}-containing pipette solutions. Each *circle* plots the increase in amplitude of I_{Cl} over this time for a different cell, normalized by the C_m of that cell. *Horizontal bars* plot the mean of values for each pipette solution [mean ± SD; 2.6 ± 2.3; $n = 7$ cells for $[Zn^{2+}]_{pip} = 0$ nM (*open circles*); 1.1 ± 0.6; $n = 6$ for $[Zn^{2+}]_{pip} = 30$ nM (*filled circles*)].

Zn^{2+} has been detected in the cytoplasm of various central neurons (Frederickson, 1989) and because EGTA binds Zn^{2+} with a greater affinity than it does other divalent cations (e.g., Ca^{2+} and Mg^{2+}; see Materials and Methods). A first test of this possibility was made by including Zn^{2+} in the pipette solution used in ruptured-patch mode. When Zn^{2+} was included in the pipette solution at a free concentration calculated to be 30 nM, the density of I_{Cl} (measured at 12–15 min after membrane rupture) ranged from 0.3 to 1.8 pA/pF (mean ± SD; 1.1 ± 0.6; $n = 6$). Without an exogenous supplement of Zn^{2+}, I_{Cl} density ranged from 0.5 to 7.2 pA/pF (mean ± SD; 2.6 ± 2.3; $n = 7$; Fig. 3*C*). The variance of the current densities measured with the Zn^{2+}-free pipette solution was significantly larger than that measured with the Zn^{2+}-containing pipette solution ($p < 0.01$, *F* test), suggesting that the growth of I_{Cl} was often facilitated by the replacement of cytoplasmic constituents by a Zn^{2+}-free solution and that this growth was hindered by the inclusion of Zn^{2+} in the pipette solution. Large increases in I_{Cl} were not observed with pipette solutions containing a calculated free Zn^{2+} concentration of 3 nM ($n = 2$). However, I_{Cl} densities were not compared in detail at different pipette Zn^{2+} concentrations because we had no means to ascertain the Zn^{2+} levels established within cells during the recordings attempted here. Under both conditions studied (30 nM vs no free Zn^{2+}), the difference between currents measured before and after DIDS application displayed outward rectification, rapid activation, no inactivation, and no time-dependent deactivation.

A second test of whether the availability of cytoplasmic Zn^{2+} abated the growth of I_{Cl} was made by superfusing cells with the membrane-permeable Zn^{2+}-selective chelator TPEN (Arslan et al., 1985) in perforated-patch mode. At 10 μM, TPEN increased the amplitude of the total whole-cell current at a test potential of +40 mV (Fig. 4*A*,*E*). The TPEN-augmented difference current (obtained by subtraction of currents recorded before and after application of TPEN) was indistinguishable from I_{Cl} in that it rectified outwardly, reversed direction at −27 ± 3 mV (when E_{Cl} was −32 mV; $n = 5$; see Fig. 4 for details), and lacked the inward tail component recorded both in the presence and absence of DIDS (Fig. 1*A*). This effect of TPEN was prevented by coapplication (of TPEN) with Zn^{2+} (Fig. 4*C*,*D*), as expected because TPEN is membrane impermeant when it has complexed with Zn^{2+} (Arslan et al., 1985).

A third test of the effect of cytoplasmic Zn^{2+} on I_{Cl} was made by microperfusing a mixture of Zn^{2+} plus an ionophore that conducts Zn^{2+} onto cells during recordings in perforated-patch mode. As shown in Figure 5*A*, the amplitude of outward current activated at a test potential of +40 mV declined in amplitude (Fig. 5*A*,*B*,*E*) after the coapplication of 1–100 μM Zn^{2+} either with 4-BrA23187 [10 μM (Erdahl et al., 1996)] or with pyrithione [20–100 μM (Zalewski et al., 1993)]. When coapplied with 4-BrA23187, 1 μM Zn^{2+} ($n = 3$), 10 μM Zn^{2+} ($n = 5$), and 100 μM Zn^{2+} ($n = 3$) produced declines of similar amplitude. Neither Zn^{2+} nor 4-BrA23187 alone reduced I_{total} at the concentrations used here, and moreover, similar declines in I_{total} were produced by the coapplication of Zn^{2+} and 4-BrA23187 when the coapplication was preceded by an application of Zn^{2+} alone ($n = 8$) or of 4-BrA23187 alone ($n = 3$). This suggests that the decline in I_{total} resulted from rises in intracellular Zn^{2+} concentration and not from a 4-BrA23187–mediated influx of Ca^{2+} or from an effect of Zn^{2+} on the external membrane surface. The zinc-damped difference current obtained by subtraction of currents recorded before and after these treatments was indistinguishable from I_{Cl} in that it rectified outwardly, reversed direction close to E_{Cl} (Fig. 5*F*), and displayed no time-dependent deactivation. The decline produced by coapplication of Zn^{2+} and pyrithione was small (0.5 pA/pF; $n = 2$) and not examined in detail.

Downward regulation of I_{Cl} by an endogenous, zinc-dependent PKC

The results described in the preceding section suggest that the amplitude of whole-cell I_{Cl} is downwardly regulated, either directly or indirectly, by cytoplasmic Zn^{2+}. We tested the possibility that this effect is exerted indirectly for four reasons: (1) because studies of direct Zn^{2+} effects on Cl^- channels in other cell types used substantially higher Zn^{2+} concentrations than those used here (see introductory remarks), (2) because biochemical assays have shown that (aside from modulating ion channel activities) Zn^{2+} facilitates PKC activity (e.g., Murakami et al., 1987; Csermely et al., 1988), (3) because PKC has been found to modulate Cl^- currents in a variety of cells (e.g., Madison et al., 1986; Li et al., 1989; Kokubun et al., 1991; Tricarico et al., 1991; Kawasaki et al., 1994; Staley, 1994; Coca-Prados et al., 1995; Duan et al., 1997), and (4) because PKC has been localized by immunocytochemical methods to retinal ganglion cells of the species used here (Osborne et al., 1992). We therefore tested

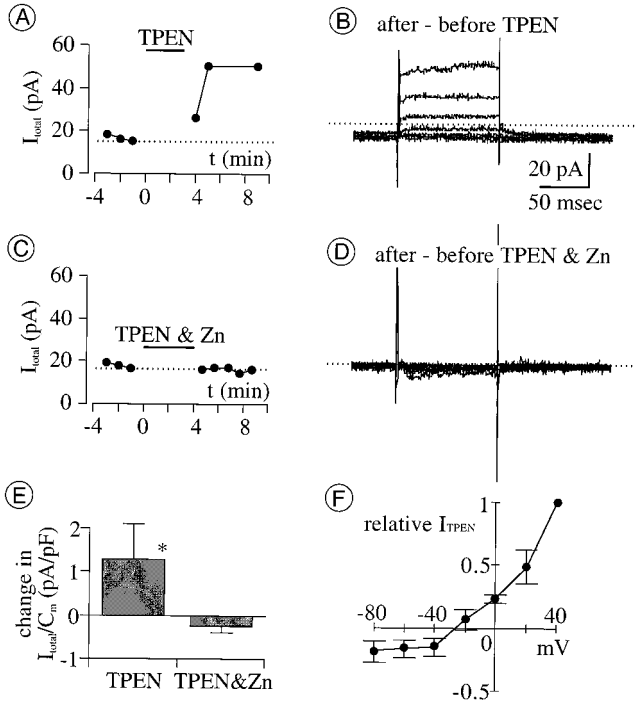

Figure 4. The membrane-permeable Zn chelator TPEN augments total whole-cell current (I_{total}). *A*, Amplitude of I_{total} activated by depolarization from −70 to +40 mV, in perforated-patch mode, before and after application of TPEN (10 μM; indicated by *horizontal bar*) is shown. Here and in all subsequent figures, application of the test agent of interest begins at 0 min; current measurements before 0 min (with or without conditioning agents) are plotted against negative time values. Note that the increase in current peaks at 6–8 min after TPEN application begins. *B*, Difference between currents activated before and after TPEN at test potentials between −80 and +40 mV is shown. *C*, *D*, TPEN (10 μM) fails to augment I_{total} when coapplied with equimolar Zn^{2+}. *E*, The current density change produced by TPEN and by a mixture of TPEN and Zn^{2+} at +40 mV is shown. Current density measured 8 min after drug application began, minus that at 1 min before drug application, is plotted (*filled vertical bars* and error bars plot mean ± 1 SEM, respectively; n = 5 for each treatment). The mean change with TPEN is significantly larger than that with TPEN and Zn^{2+} (*p = 0.0216). *F*, *I–V* relation of TPEN-augmented current is shown (*filled circles* and error bars plot mean ± SEM, respectively; n = 5). Amplitude is normalized to the value at +40 mV and plotted against test potential. E_{rev}, −27 ± 3 mV; E_{Cl}, −32 mV. In all panels, currents were recorded in the control bath solution before TPEN application. TPEN was then superfused for 3–4 min after replacing the bath Co^{2+} with Ca^{2+} (because TPEN binds Co^{2+} more than Ca^{2+} and only unbound TPEN can pass through cell membranes). Effects of TPEN were assessed by recording currents after replacing the TPEN- and Ca^{2+}-containing solution with control (Co^{2+}-containing) solution to bind residual TPEN (if any) and to block voltage-gated Ca^{2+} currents.

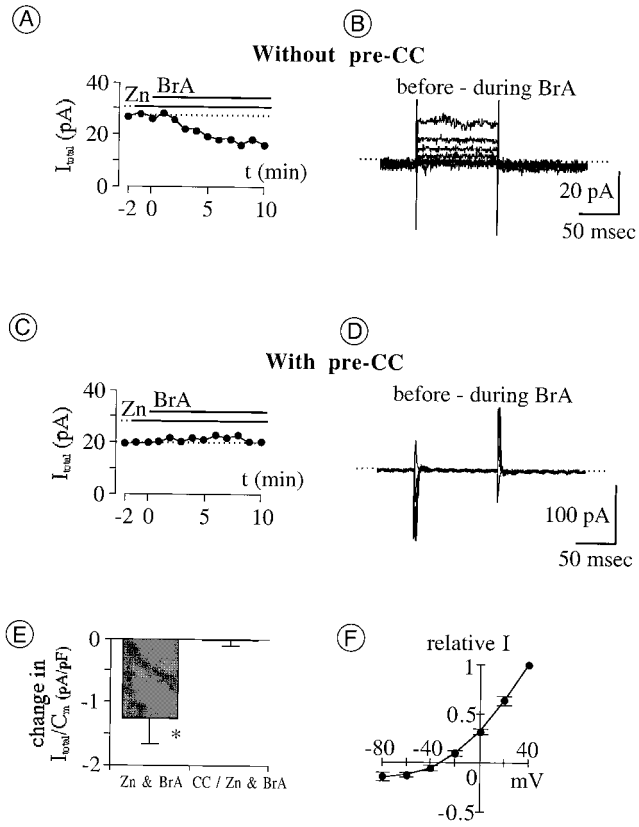

Figure 5. Effects of Zn^{2+} "loading" and PKC inhibition on total whole-cell current (I_{total}) in perforated-patch mode. The cytoplasmic Zn^{2+} level was raised by extracellular application (indicated by *horizontal bars*) of $ZnCl_2$ (*Zn*) together with the Zn^{2+}-preferring ionophore 4-BrA23187 (*BrA*). Endogenous PKC was blocked by preincubation with calphostin C (*CC*). *A*, *C*, Amplitude of I_{total} at +40 mV plotted against recording time. Each *panel* is from a single cell. The *dotted line* indicates current level before coapplication of *Zn* and *BrA*. *A*, Sequential application of 100 μM *Zn* and 10 μM *BrA*. I_{total} begins to decline after coapplication commences (at t = 0 min); within the next 8 min, current reduction is maximal. *C*, Sequential application of 10 μM *Zn* and 10 μM *BrA*, preceded by a 30 min preincubation in 1 μM *CC*. I_{total} remains constant during the 10 min coapplication of *Zn* and *BrA*. *B*, *D*, Difference between I_{total} recorded 1 min before and 10 min after coapplication of *Zn* and *BrA*. Current *traces* in *B* and *D* are from cells in *A* and *C*, respectively. The voltage protocol is as described in Figure 1 (E_{hold}, −70 mV; E_{test}, −80 to +40 mV; 20 mV steps). *E*, Reduction in I_{total} after 10 min coapplication of *Zn* and *BrA*, with and without 30 min preincubation in 1 μM *CC*. *Filled vertical bars* and error bars plot the mean and SEM, respectively, of the reduction in current amplitude at +40 mV, divided by C_m to normalize for cell size. Current reduction by *Zn* is significantly greater without *CC* than with *CC* (*p = 0.0058), indicating that reduction of I_{Cl} by *Zn* can be blocked by inhibition of endogenous PKC. *CC*/*Zn & BrA*, Coapplication of 10 μM *Zn* and 10 μM *BrA* after preincubation (n = 5); *Zn & BrA*, coapplication of 1–10 μM *Zn* and 10 μM *BrA* without preincubation (n = 7). *F*, *I–V* curve of current reduced by coapplication of *Zn* (1–10 μM) and *BrA* (10 μM). *Filled circles* plot the mean of difference current amplitudes measured as described in *B* (n = 6). Means are normalized to the value at +40 mV. Error bars indicate 1 SEM. E_{rev}, −34.5 ± 5 mV.

whether I_{Cl} is regulated by endogenous PKC activity and whether this control was zinc dependent.

We first tested the effect of extracellularly applied PKC inhibitors on I_{Cl} in perforated-patch mode. Both agents tested (0.1–1 μM calphostin C and 1 μM bisindolylmaleimide I) (cf. Shapiro et al., 1996) produced an increase in the amplitude of the total outward current (n = 4 for each agent; Fig. 6*G*). At a test potential of +40 mV, current amplitude increased noticeably (e.g., by 10–20%) over the control value within 4–8 min after application of either agent (Fig. 6*A*,*C*). Current amplitude continued to increase thereafter during applications of either agent for as long as 10–15 min. We infer that increases in the amplitude of I_{Cl} account for most (if not all) of the increases in outward current observed, because the latter were reduced by DIDS (1 mM) and because the kinetics and voltage sensitivity of the difference current traces obtained by subtraction of currents recorded before and after exposure to PKC inhibitors (Fig. 6*B*,*D*,*H*) resemble those of the Cl^- current described above (Fig. 1). These results suggest that I_{Cl} is reduced in resting retinal ganglion cells by an endogenous PKC activity.

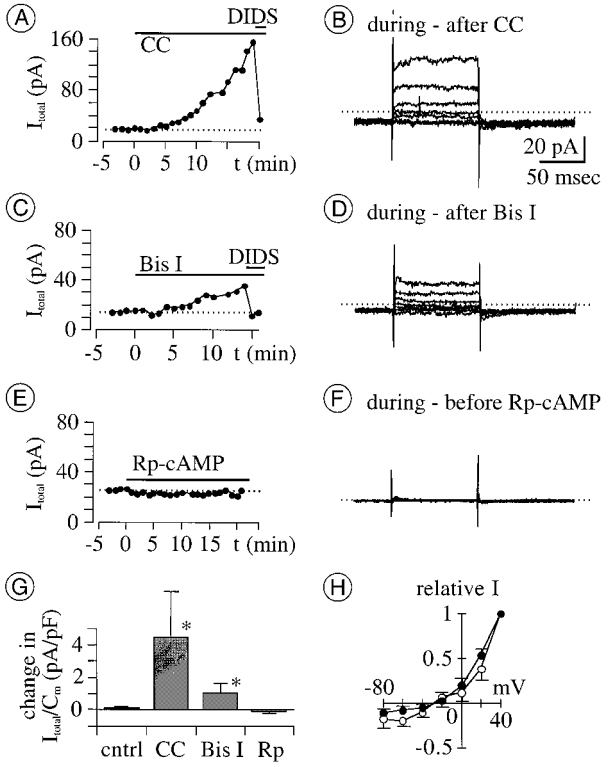

Figure 6. Effect of membrane-permeable PK inhibitors on I_{Cl} in perforated-patch mode. *A*, *C*, *E*, Amplitude of total current (I_{total}) at +40 mV before and after application (indicated by *horizontal bars*) of inhibitors of PKC and PKA. Each recording is from a different cell. Concentrations used were 0.1 μM calphostin C (*CC*), 1 mM DIDS, 1 μM bisindolylmaleimide I (*Bis I*), and 0.1 mM Rp-cAMP. Amplitudes of I_{total} start to increase 4–8 min after *CC* (*A*) and *Bis I* (*C*) applications begin, and grow continuously and gradually thereafter. DIDS (applied at times indicated by *short horizontal bars*) reduces current toward the levels before *CC* and *Bis I*. *B*, *D*, *F*, Difference between currents recorded before and after 13–21 min application of various test agents. Data in *B*, *D*, and *F* were obtained from the same cells shown in *A*, *C*, and *E*, respectively. Calibration (in *B*) is the same in all *panels*. The kinetics of difference currents in *B* and *D* (i.e., of currents augmented by *CC* and by *Bis I*) resembles those of I_{Cl} in Figure 1. *G*, Mean change in density of I_{total} at +40 mV after 15–20 min application of various test agents. *Bis I*, 1 μM *Bis I*; *CC*, 0.1–1 μM *CC*; *cntrl*, control bath solutions supplemented with vehicle (DMSO) only; *Rp*, 0.1–1 mM Rp-cAMP ($n = 4$ for each treatment). The mean change with *CC* and *Bis I* is significantly larger than the control level ($^*p > 0.0209$ for both). *H*, *I–V* relation of current augmented by *CC* (*filled circles*) and *Bis I* (*open circles*). Amplitude was normalized to the maximum value recorded from each cell at +40 mV and plotted against test potential. *Symbols* and error bars plot the mean ± SEM, respectively ($n = 4$ for each treatment). Voltage sensitivity of these currents resembles those of I_{Cl} in Figure 1. E_{rev} of *CC*- and *Bis I*-augmented currents, −27 ± 8 and −28 ± 3 mV, respectively; E_{Cl}, −32 mV.

As might therefore be expected, DIDS-sensitive current was undetectably small when PKC catalytic subunit (~4 pM) was included in pipette solutions during ruptured-patch recordings ($n = 5$; Fig. 7*A*). Moreover, DIDS-sensitive current (I_{Cl}) could be activated when a PKC inhibitor (PKC[19–31]) (cf. Lin et al., 1994) and PKC catalytic subunit were included together in the pipette solution during ruptured-patch recordings ($n = 5$ for each treatment; Fig. 7). Therefore, the observed reduction of I_{Cl} amplitude cannot be ascribed to nonspecific effects of the PKC catalytic subunit (i.e., effects beside phosphorylation).

Lastly, we tested whether the downward regulation of I_{Cl} by endogenous PKC and that by cytoplasmic Zn^{2+} were linked. This was done by measuring I_{total} in the presence of calphostin C, Zn^{2+}, and 4-BrA23187. Figure 5, *C* and *E*, shows that 10 μM Zn^{2+} and 10 μM 4-BrA23187 did not reduce the amplitude of I_{total} in cells incubated for 30 min in 1 μM calphostin C. The subtraction of currents recorded in the presence of all three agents from those recorded in the presence of Zn^{2+} and calphostin C alone showed no measurable difference current at any of the test potentials used ($n = 5$; Fig. 5*D*; only slight changes in capacitive current artifacts are seen at the onset and offset of the test potentials). The current reduction by Zn^{2+} was significantly less after ≥30 min preincubations with calphostin C than without it (Fig. 5*E*; $p = 0.0058$), indicating that inhibition of endogenous PKC impeded the reduction of I_{Cl} by Zn^{2+}. Consistent with this and with the lag observed between calphostin C application and I_{Cl} augmentation (e.g., Fig. 6), I_{Cl} amplitude grew monotonically if 10 μM Zn^{2+} and 10 μM 4-BrA23187 were coapplied after a 10 min (rather than 30 min) exposure to 1 μM calphostin C ($n = 5$; data not shown). All of these results would be expected if the reduction of I_{Cl} by cytoplasmic Zn^{2+} (like that shown in Fig. 5*A*) was mediated by PKC.

Under the same recording conditions in which PKC inhibitors increased I_{Cl}, the Rp-isomer of cAMP (0.1–1 mM) produced no detectable change in I_{Cl} when applied onto cells by microperfusion for as long as 25 min (Fig. 6*G*,*H*). Because Rp-cAMP is a membrane-permeable inhibitor of protein kinase A (PKA) and because the concentrations used are 10–100 times greater than its K_i, we did not further test whether endogenous PKA activity regulates I_{Cl}.

DISCUSSION

We have described here an outwardly rectifying Cl^- current (I_{Cl}) whose amplitude appears to be downwardly regulated in a zinc-dependent manner by an endogenous PKC. Below, we discuss the role of zinc in suppressing this current, compare this current with anionic conductances in other cells, and delimit speculation about the function of this current.

Indirect effects of Zn^{2+}

Previous studies showed that the open time of outward single-channel Cl^- currents is reduced by application of 1–10 mM Zn^{2+} to the cytoplasmic side of isolated membrane patches and interpreted these effects as resulting from a voltage-dependent block (Woll et al., 1987; Kokubun et al., 1991; Groschner and Kukovetz, 1992). Our results might seem similar in that exposure of cells to Zn^{2+} and either 4-BrA23187 or pyrithione reduced the amplitude of outward whole-cell Cl^- current (Fig. 5). However, our results differ from these previous reports in at least three respects. First, both inward and outward Cl^- current amplitudes were augmented by pharmacological treatments that chelate cytoplasmic Zn^{2+} (exposure to TPEN; buffering divalent cation levels in nominally Zn^{2+}-free ruptured-patch pipette solutions with EGTA); conversely, both currents were reduced by treatments designed to augment intracellular Zn^{2+} levels (Figs. 3*A*, 4*B*, 5*B*). These results are not readily explained by assuming a voltage-dependent block by Zn^{2+} like that considered in the outward Cl^- current measurements cited above. Second, inclusion of 30 nM free Zn^{2+} in our pipette solutions was effective in minimizing Cl^- current increases in the ruptured-patch recording mode. This implies that I_{Cl} may be controlled by Zn^{2+} concentrations several orders of magnitude lower than those applied in the studies cited above (without excluding the possibility that higher

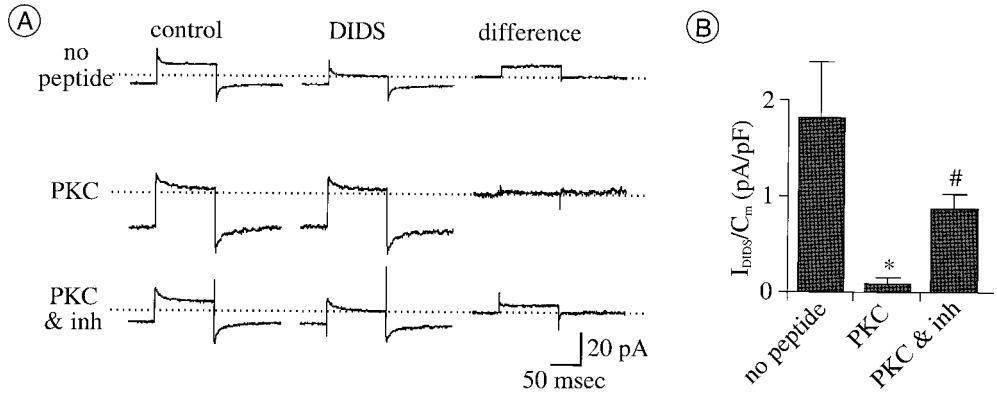

Figure 7. Downregulation of I_{Cl} by PKC-mediated phosphorylation. *A*, Currents activated by depolarization from −70 to +40 mV before (*left column*) and during (*middle column*) application of 1 mM DIDS and with digital subtractions thereof (*right column*). Each *row* of currents is from a separate cell, with the ruptured-patch pipette solution containing no peptide (*top row*), 4 pM PKC catalytic subunit (*middle row*), or a mixture of 4 pM PKC catalytic subunit and PKC inhibitor [1 μM PKC(19–31)] (*bottom row*). DIDS was applied to each cell 9–15 min after formation of ruptured-patch–recording mode. The *flat* difference current in the *middle row* shows that there is no current blocked by DIDS in the presence of PKC. The DIDS-sensitive difference current in the *bottom row* shows I_{Cl} spared by PKC inhibition. *B*, Density of DIDS-sensitive currents measured as described in *A*. *Filled vertical bars* and error bars plot the mean ± SEM; $n = 5$ for each treatment. In each recording, the pipette solution contained 2 mM ATP and no added Zn^{2+}. Mean density is significantly reduced by PKC from the control (no peptide) level ($^*p = 0.0122$). Mean density with PKC(19–31) is significantly larger than those with PKC only ($\#p = 0.0122$).

Zn^{2+} concentrations might hinder Cl^- channel gating in retinal ganglion cells) (cf. Staley, 1994). Third, we found that the effect of exogenously supplied cytoplasmic Zn^{2+} was blocked by the PKC inhibitor calphostin C. This suggests that I_{Cl} was not inhibited by Zn^{2+} alone. If increased cytoplasmic Zn^{2+} levels reduced I_{Cl} independently of PKC in our recordings, then these decreases were so small that they were outweighed by the increases in I_{Cl} produced by PKC inhibition (Fig. 5*E*).

The similarly slow and marked growth in Cl^- current amplitude we observed after exposure to calphostin C and bisindolylmaleimide I, superfusion with TPEN, and internal perfusion with EGTA (without added Zn^{2+}) would all be expected if I_{Cl} was downregulated by a PKC whose activity depends on Zn^{2+}. Alone, any one of these results would have corroborated the results of previous studies, as Cl^- current blockade by Zn^{2+} at the cytoplasmic side of membranes and the downward regulation of Cl^- current by PKC have been described separately in other preparations (cited both above and below). Furthermore, PKC has been localized immunocytochemically to retinal ganglion cells in all species examined to date (e.g., Cuenca et al., 1990; Usuda et al., 1991; Osborne et al., 1992; Kolb et al., 1993; Fukuda et al., 1994). To our knowledge, however, the zinc dependence of the downward regulation of a Cl^- current by PKC that we report here is novel. For that matter, our study provides the first electrophysiological evidence consistent with biochemical measurements of zinc-dependent PKC activity in other systems (Murakami et al., 1987; Csermely et al., 1988; Hubbard et al., 1991). This possibility was not predictable from immunocytochemical studies, as several PKC isozymes have been localized to retinal ganglion cells (e.g., Usuda et al., 1991; Osborne et al., 1992; Kolb et al., 1993), Zn^{2+} has not been detected anatomically in retinal ganglion cells (Ugarte and Osborne, 1998), and Zn^{2+} that is bound to PKC would not be detectable by any anatomical methods that we are aware of (Frederickson, 1989; Sensi et al., 1997). However, one of the PKC isozymes (PKC-β) localized to retinal ganglion cells of the species used in this study (Osborne et al., 1992) is a type whose activity has been shown by biochemical methods to be zinc dependent (Murakami et al., 1987; Csermely et al., 1988; Hubbard et al., 1991). Our results provide independent evidence of such activity, and in the absence of other candidates, we provisionally attribute the PKC- and zinc-dependent regulation of Cl^- current to this isozyme. This possibility could be of general interest because PKC-β has also been localized in frog, turtle, rabbit, monkey, and human retinal ganglion cells (Cuenca et al., 1990; Usuda et al., 1991; Osborne et al., 1992; Kolb et al., 1993; Fukuda et al., 1994).

Cl^- current identification

Four types of Cl^- current have been found previously to be reduced in amplitude by PKC activity. However, none of these currents are known to have all of the properties we report here. The Cl^- current blocked by PKC activation in hippocampal pyramidal cells is activated by hyperpolarization and rectifies inwardly (Madison et al., 1986; Staley, 1994); large single-channel anion currents recorded after PKC inhibition or membrane patch excision (Kokubun et al., 1991; Groschner and Kukovetz, 1992) display bell-shaped activation curves; Cl^- channels are inactivated by PKC in normal and cystic fibrosis airway epithelia, but only at cytoplasmic Ca^{2+} concentrations >150 nM (Li et al., 1989); and background Cl^- currents that are reduced by PKC in other preparations [skeletal muscle (Tricarico et al., 1991); renal and cardiac ClC-3 channels (Kawasaki et al., 1994; Duan et al., 1997); and ciliary epithelium (Coca-Prados et al., 1995)] have yet to be examined for cytoplasmic Zn^{2+} sensitivity. Cytoplasmic Ca^{2+} inhibits ClC-3 channel currents (Kawasaki et al., 1995) at levels that did not noticeably alter the I_{Cl} reported here. However, the significance of this difference remains to be investigated, because the inhibition by Ca^{2+} was observed under conditions unlike ours (in the presence of a protein kinase inhibitor and alkaline phosphatase, and in the absence of ATP and Zn^{2+}) and because we have been unable to make stable whole-cell recordings from retinal ganglion cells in hypotonic or isotonic bath solutions (see Materials and Methods).

The background I_{Cl} we have found in retinal ganglion cells also appears to be distinct from all five types of Cl^- current described in other retinal cells. I_{Cl} was not detectably affected by cytoplasmic Ca^{2+} levels buffered (nominally) to between 3 and 300 nM and thus differs from the Ca^{2+}-activated Cl^- current of photoreceptor and bipolar cells (see Results). In addition, I_{Cl} was not blocked by picrotoxinin and thus differs from Cl^- channels complexed with $GABA_A$, $GABA_C$, and glycine receptors (see Wang et al., 1995). Lastly, I_{Cl} was not affected by Rp-cAMP and thus differs from the Cl^- conductance in pigmented epithelial cells (Peterson et al., 1997). Coincidentally, protein kinase activities

have been found to reduce the amplitude of sustained Cl^- currents found so far in all retinal cells, regardless of the conditions under which they activate [resting voltage (Fig. 1) or exposure to GABA (Feigenspan and Bormann, 1994), glycine (Han and Slaughter, 1998), and cytoplasmic Ca^{2+} (Peterson et al., 1997)].

Cl^- current function

Our results indicate that retinal ganglion cells possess at least two resting ion conductances. One is permeable to K^+ ions (Bindokas et al., 1994), whereas the other is the Cl^- conductance reported here. Like the ohmic conductance recorded between −105 and −55 mV in the absence of extracellular K^+ ions (Tabata and Ishida, 1996), I_{Cl} showed no time-dependent activation, inactivation, or deactivation. On the other hand, the relatively small density of I_{Cl} near resting potential and its nonlinear dependence on voltage are characteristic of background Cl^- currents in various tissues (Franciolini and Petris, 1990). Regardless of its gating mechanism, I_{Cl} was consistently detected at test potentials as negative as −80 mV, suggesting that I_{Cl} is tonically activated *in situ* at membrane voltages at least as negative as the resting potential.

Because resting potential is relatively close to the K^+ equilibrium potential, even if the Cl^- equilibrium potential is raised to 0 mV (Ishida, 1995), K^+ conductance evidently contributes more to resting potential than the Cl^- conductance reported here (see also Ascher et al., 1976). However, our results imply that the contribution of I_{Cl} to resting potential and other electrical properties of cells (membrane time constant, input impedance, and synaptic integration) might not be fixed. Conceivably, these contributions could be augmented or diminished, given our observation that the Cl^- permeability rises if recording conditions deplete cytoplasmic Zn^{2+} or inhibit PKC and that its resting level can be decreased by treatments that augment cytoplasmic Zn^{2+}. Moreover, these contributions could be altered slowly and persistently by synaptic modulation of PKC activity, because I_{Cl} showed no susceptibility to inactivation by membrane potential. Lastly, because we recorded I_{Cl} at membrane potentials that are more negative and more positive than typical resting potentials, and because retinal ganglion cells are inhibited by GABA- and glycine-gated Cl^- conductances *in situ*, a background Cl^- permeability may provide retinal ganglion cells with a means of reducing the driving force for Cl^- currents (and thus, of reducing membrane potential fluctuations) without obviating shunting types of inhibition. Until more is known about PKC regulation and the distribution of I_{Cl} within retinal ganglion cells *in situ*, we refrain from further speculation about its possible functions.

REFERENCES

Arslan P, Di Virgilio F, Beltrame M, Tsien RY, Pozzan T (1985) Cytosolic Ca^{2+} homeostasis in Ehrlich and Yoshida carcinomas. J Biol Chem 260:2719–2727.

Ascher P, Kunze D, Neild TO (1976) Chloride distribution in *Aplysia* neurones. J Physiol (Lond) 256:441–464.

Bader CR, Bertrand D, Schwartz EA (1982) Voltage-activated and calcium-activated currents studied in solitary rod inner segments from the salamander retina. J Physiol (Lond) 331:253–284.

Begenisich T, Lynch C (1974) Effects of internal divalent cations on voltage-clamped squid axons. J Gen Physiol 63:675–689.

Bindokas VP, Yoshikawa M, Ishida AT (1994) Na^+-Ca^{2+} exchanger-like immunoreactivity and regulation of intracellular Ca^{2+} levels in fish retinal ganglion cells. J Neurophysiol 72:47–55.

Brocard JB, Rajdev S, Reynolds IJ (1993) Glutamate-induced increases in intracellular free Mg^{2+} in cultured cortical neurons. Neuron 11:751–757.

Brooks SPJ, Storey KB (1992) Bound and determined: a computer program for making buffers of defined ion concentrations. Anal Biochem 201:119–126.

Burgoyne RD, Morgan A (1995) Ca^{2+} and secretory-vesicle dynamics. Trends Neurosci 18:191–196.

Callahan MJ, Korn SJ (1994) Permeation of Na^+ through a delayed rectifier K^+ channel in chick dorsal root ganglion neurons. J Gen Physiol 104:747–771.

Chang D, Hsieh PS, Dawson DC (1988) Calcium: a program in BASIC for calculating the composition of solutions with specified free concentrations of calcium, magnesium and other divalent cations. Comput Biol Med 18:351–366.

Coca-Prados M, Anguita J, Chalfant KL, Civan MM (1995) PKC-sensitive Cl^- channels associated with ciliary epithelial homologue of pI_{Cln}. Am J Physiol 268:C572–C579.

Csermely P, Szamel M, Resch K, Somogyi J (1988) Zinc can increase the activity of protein kinase C and contributes to its binding to plasma membranes in T lymphocytes. J Biol Chem 263:6487–6490.

Cuenca N, Fernandez E, Kolb H (1990) Distribution of immunoreactivity to protein kinase C in the turtle retina. Brain Res 532:278–287.

Duan D, Winter C, Cowley S, Hume JR, Horowitz B (1997) Molecular identification of a volume-regulated chloride channel. Nature 390:417–421.

Erdahl WL, Chapman CJ, Wang E, Taylor RW, Pfeiffer DR (1996) Ionophore 4-BrA23187 transports Zn^{2+} and Mn^{2+} with high selectivity over Ca^{2+}. Biochemistry 35:13817–13825.

Etter EF, Minta A, Poenie M, Fay FS (1996) Near-membrane $[Ca^{2+}]$ transients resolved using the Ca^{2+} indicator FFP18. Proc Natl Acad Sci USA 93:5368–5373.

Feigenspan A, Bormann J (1994) Modulation of $GABA_c$ receptors in rat retinal bipolar cells by protein kinase C. J Physiol (Lond) 481:325–330.

Forbes IJ, Zalewski PD, Giannakis C (1991) Role for zinc in a cellular response mediated by protein kinase C in human B lymphocytes. Exp Cell Res 195:224–229.

Franciolini F, Petris A (1990) Chloride channels of biological membranes. Biochim Biophys Acta 1031:247–259.

Frederickson CJ (1989) Neurobiology of zinc and zinc-containing neurons. Int Rev Neurobiol 31:145–238.

Fukuda K, Saito N, Yamamoto M, Tanaka C (1994) Immunocytochemical localization of the α, βI, βII- and γ-subspecies of protein kinase C in the monkey visual pathway. Brain Res 658:155–162.

Groschner K, Kukovetz WR (1992) Voltage-sensitive chloride channels of large conductance in the membrane of pig aortic endothelial cells. Pflügers Arch 421:209–217.

Hamill OP, Marty A, Neher E, Sakmann B, Sigworth FJ (1981) Improved patch-clamp techniques for high-resolution current recording from cells and cell free patches. Pflügers Arch 391:85–100.

Han Y, Slaughter MM (1998) Protein kinases modulate two glycine currents in salamander retinal ganglion cells. J Physiol (Lond) 508:681–690.

Hidaka S, Ishida AT (1998) Voltage-gated Na^+ current availability after step- and spike-shaped conditioning depolarizations of retinal ganglion cells. Pflügers Arch 436:497–508.

Holevinsky KO, Jow F, Nelson DJ (1994) Elevation in intracellular calcium activates both chloride and proton currents in human macrophages. J Membr Biol 140:13–30.

Horn R, Marty A (1988) Muscarinic activation of ionic currents measured by a new whole-cell recording method. J Gen Physiol 94:145–159.

Hubbard SR, Bishop WR, Kirschmeier P, George SJ, Cramer SP, Hendrickson WA (1991) Identification and characterization of zinc binding sites in protein kinase C. Science 254:1776–1779.

Ishida AT (1995) Ion channel components of retinal ganglion cells. Prog Retin Eye Res 15:261–280.

Johnson BD, Byerly L (1993) A cytoskeletal mechanism for Ca^{2+} channel metabolic dependence and inactivation by intracellular Ca^{2+}. Neuron 10:797–804.

Johnson JW, Ascher P (1990) Voltage-dependent block by intracellular Mg^{2+} of *N*-methyl-D-aspartate-activated channels. Biophys J 57:1085–1090.

Kawasaki M, Uchida S, Monkawa T, Miyawaki A, Mikoshiba K, Marumo F, Sasaki S (1994) Cloning and expression of a protein kinase C-regulated chloride channel abundantly expressed in rat brain neuronal cells. Neuron 12:597–604.

Kawasaki M, Suzuki M, Uchida S, Sasaki S, Marumo F (1995) Stable

and functional expression of the ClC-3 chloride channel in somatic cell lines. Neuron 14:1285–1291.
Kokubun S, Saigusa A, Tamura T (1991) Blockade of Cl channels by organic and inorganic blockers in vascular smooth muscle cells. Pflügers Arch 418:204–213.
Kolb H, Zhang L, Dekorver L (1993) Differential staining of neurons in the human retina with antibodies to protein kinase C isozymes. Vis Neurosci 10:341–351.
Lascola CD, Nelson DJ, Kraig RP (1998) Cytoskeletal actin gates a Cl^- channel in neocortical astrocytes. J Neurosci 18:1679–1692.
Li M, McCann JD, Anderson MP, Clancy JP, Liedtke CM, Nairn AC, Greengard P, Welsh MJ (1989) Regulation of chloride channels by protein kinase C in normal and cystic fibrosis airway epithelia. Science 244:1353–1356.
Lin YF, Browning MD, Dudek EM, MacDonald RL (1994) Protein kinase C enhances recombinant bovine α1-β1-γ2L GABA(A) receptor whole-cell currents expressed in L929 fibroblasts. Neuron 13:1421–1431.
Lukasiewicz PD, Werblin FS (1988) A slowly inactivating potassium current truncates spike activity in ganglion cells of the tiger salamander retina. J Neurosci 8:4470–4481.
Madison DV, Malenka RC, Nicoll RA (1986) Phorbol esters block a voltage-sensitive chloride current in hippocampal pyramidal cells. Nature 321:695–697.
Maricq AV, Korenbrot JI (1988) Calcium and calcium-dependent chloride currents generate action potentials in solitary cone photoreceptors. Neuron 1:503–515.
Marks PW, Maxfield FR (1991) Preparation of solutions with free calcium concentration in the nanomolar range using BAPTA. Anal Biochem 193:61–71.
Matsuda H, Saigusa A, Irisawa H (1987) Ohmic conductance through the inwardly rectifying K channel and blocking by internal Mg^{2+}. Nature 325:156–159.
Murakami K, Whiteley MK, Routtenberg A (1987) Regulation of protein kinase C activity by cooperative interaction of Zn^{2+} and Ca^{2+}. J Biol Chem 262:13902–13906.
Okada T, Horiguchi H, Tachibana M (1995) Ca^{2+}-dependent Cl^- current at the presynaptic terminals of goldfish retinal bipolar cells. Neurosci Res 23:297–303.
O'Rourke B, Backx PH, Marban E (1992) Phosphorylation-independent modulation of L-type calcium channels by magnesium-nucleotide complexes. Science 257:245–248.
Osborne NN, Barnett NL, Morris NJ, Huang FL (1992) The occurrence of three isozymes of protein kinase C (α, β and γ) in retinas of different species. Brain Res 570:161–166.
Peterson WM, Quong JN, Blaug SA, Miller SS (1997) Evidence that cyclic-AMP dependent chloride conductance is controlled by phospholamban rather than CFTR on bovine RPE. Invest Ophthalmol Vis Sci 38:s467.
Roberts WM (1993) Spatial calcium buffering in saccular hair cells. Nature 363:74–76.
Sekiguchi K, Tsukuda M, Ase K, Kikkawa U, Nishizuka Y (1988) Mode of activation and kinetic properties of three distinct forms of protein kinase C from rat brain. J Biochem (Tokyo) 103:759–765.
Sensi SL, Canzoniero LMT, Yu SP, Ying HS, Koh J-Y, Kerchner GA, Choi DW (1997) Measurement of intracellular free zinc in living cortical neurons: routes of entry. J Neurosci 17:9554–9564.
Shapiro MS, Zhou J, Hille B (1996) Selective disruption by protein kinases of G-protein-mediated Ca^{2+} channel modulation. J Neurophysiol 76:311–320.
Smith RM, Martell AE (1975) Critical stability constants. New York: Plenum.
Staley K (1994) The role of an inwardly rectifying chloride conductance in postsynaptic inhibition. J Neurophysiol 72:273–284.
Stelzer A, Kay AR, Wong RKS (1988) $GABA_A$-receptor function in hippocampal cells is maintained by phosphorylation factors. Science 241:339–341.
Sucher NJ, Lipton SA (1992) A slowly inactivating K^+ current in retinal ganglion cells from postnatal rat. Vis Neurosci 8:171–176.
Tabata T, Ishida AT (1996) Transient and sustained depolarization of retinal ganglion cells by I_h. J Neurophysiol 75:1932–1943.
Tabata T, Ishida AT (1997) Intracellular zinc may sustain PKC-mediated reduction of outwardly rectifying Cl^- current in retinal ganglion cells. Soc Neurosci Abstr 23:2360.
Tricarico D, Conte Camerino D, Govoni S, Bryant SH (1991) Modulation of rat skeletal muscle chloride channels by activators and inhibitors of protein kinase C. Pflügers Arch 418:500–503.
Ugarte M, Osborne NN (1998) The localization of endogenous zinc and the *in vitro* effect of exogenous zinc on the GABA immunoreactivity and formation of reactive oxygen species in the retina. Gen Pharmacol 30:297–303.
Usuda N, Kong Y, Hagiwara M, Uchida C, Terasawa M, Nagata T, Hidaka H (1991) Differential localization of protein kinase C isozymes in retinal neurons. J Cell Biol 112:1241–1247.
Wang T-L, Hackam AS, Guggino WB, Cutting GR (1995) A single amino acid in γ-aminobutyric acid ρ1 receptors affects competitive and noncompetitive components of picrotoxin inhibition. Proc Natl Acad Sci USA 92:11751–11755.
Woll KH, Leibowitz MD, Neumcke B, Hille B (1987) A high-conductance anion channel in adult amphibian skeletal muscle. Pflügers Arch 410:632–640.
Zalewski PD, Forbes IJ, Betts WH (1993) Correlation of apoptosis with change in intracellular labile Zn(II) using Zinquin [(2-methyl-8-*p*-toluenesulphonamido-6-quinolyloxy)acetic acid] a new specific fluorescent probe for Zn(II). Biochem J 296:403–408.
Zhu Y, Ikeda SR (1993) Anomalous permeation of Na^+ through a putative K^+ channel in rat superior cervical ganglion neurones. J Physiol (Lond) 468:441–461.